

AN ABSTRACT OF THE THESIS OF

Kebin Li for the **Master of Science** in **Physical Science, Physics**
Emphasis presented in **May 1996**. Title: **Convolution and Optimal**
Filtering in a Fiber Optic Detection System.

Abstract approved: George Ballantine

The Fourier transform and the general methods of linear system theory are very important in the analysis of optical imaging systems. These tools are used to analyze a double-slit intensity pattern as measured by an optical fiber bundle connected to an inexpensive PASCO photodetector. The three important functions involved in this analysis are the input intensity function to the detector, the output of the detector and the response function which characterizes the detection system. The recorded data of the intensity pattern includes the effects of both noise and modification of the detection system. We have developed methods to eliminate these two effects and obtain an unspoiled double-slit diffraction pattern. These methods are discussed with a view towards developing an improved system in the future.

Convolution and Optimal Filtering
in a
Fiber Optic Detection System

A Thesis

Presented to

the Division of Physical Sciences

EMPORIA STATE UNIVERSITY

In Partial Fulfillment of

the Requirements for the Degree

Master of Science

by

Kebin Li

May 1996

Dwayne Beckner
Approved by the Major Division

John Schum
Approved by the Graduate Council

Jose Ballata
Committee Chairman

R. Jones
Committee Member

Philip E. Gustafson
Committee Member

Acknowledgments

I would like to express my deepest gratitude to Dr. Jorge Ballester for his guidance and supervision in the completion of this research. I would also like to thank Professor James Calvert, Dr. Robert Jones, Dr. Ron Keith, Dr. Phil Gustafson and Dr. DeWayne Backhus for their invaluable advice and encouragement.

Table of Contents

Acknowledgments.....	iii
Table of Contents.....	iv
List of Figures.....	v
Chapter 1. Introduction.....	1
Chapter 2. Double-slit Diffraction Pattern Theory and Experiment.....	3
Chapter 3. Fourier Analysis and Optimal Filtering Theory.....	11
Chapter 4. Results.....	28
Chapter 5. Conclusions.....	42
References.....	43

List of Figures

Figure 1.....	4
Figure 2.....	8
Figure 3.....	9
Figure 4.....	30
Figure 5.....	31
Figure 6.....	32
Figure 7.....	33
Figure 8.....	34
Figure 9.....	36
Figure 10.....	37
Figure 11.....	38
Figure 12.....	40
Figure 13.....	41

Chapter 1

Introduction

Fourier methods have revolutionized fields of science and engineering, from radio astronomy to medical imaging, from seismology to spectroscopy. They are so important and useful now that every field dealing with wave phenomenon can use them. In the area of optical image processing, Fourier analysis is at the core of it.

Our research goal is to develop an optical fiber bundle scanning detection system as a test system. Since the measured data always includes noise and the effect of the detector, how to eliminate these two effects and regain the original pure signal is what we try to investigate.

We choose the double-slit Fraunhofer diffraction pattern to investigate the differences between the theoretical pattern which can be calculated accurately by the diffraction theory and the measured experimental data. In this way we can carefully compare them to see how the noise and detector actually affect the recorded pattern. Then we try to eliminate these effects by applying some techniques of Fourier analysis. Both our experimental work and theoretical research efforts will be presented in later chapters.

Convolution is a very important concept to understand the formation of the recorded diffraction pattern. When the input intensity pattern is received by the detector, it is convolved with the response function of the

detector which then produces the output signal. Deconvolution is the process of undoing the smearing in a data set that has occurred under the influence of a known response function. For our situation this is the result of a less-than-perfect measuring apparatus. The convolution theorem and deconvolution theorem are two very important theorems in Fourier analysis. We tried to apply them to eliminate the effect of the response of the detector.

We found that the optimal (Wiener) filtering is a technique that can be applied. Since the input intensity pattern was corrupted by noise, a consideration of the effect of the detector only by applying the deconvolution theorem failed. Because of this, optimal filtering was chosen in order to remove the noise from the corrupted output signal.

After carefully designing models for the response function of the detector and the noise, we got very good deconvolution results. The significance of this research is that we can effectively remove all the effects that corrupt the pure original signal.

In Chapter 2 we present both the theoretical calculation and the experimental results of the double-slit diffraction pattern. Chapter 3 is the basic Fourier and optimal filtering theory for the analysis. Our theoretical analysis is discussed in Chapter 4. In Chapter 5 we give our conclusions.

Chapter 2

Double-slit Diffraction Pattern Theory and Experiment

1. Theoretical Calculation of Double-slit Diffraction Pattern

The reason we choose the double-slit diffraction pattern is that it can be calculated very accurately using the Fraunhofer diffraction theory. When we consider the double-slit diffraction pattern we assume the light incident on the slits is composed of parallel rays. In the wave model of light this corresponds to plane parallel waves. Since we use a HeNe Laser as our light source, we expect a beam which is parallel to a very high degree.

²As in Figure 1, the situation consists of two long slits of width b and center-to-center separation a . The total light intensity is projected on a screen or other surface which is a distance D from the slits. In order to use Fraunhofer diffraction theory, D should be relatively large, i.e., $D \gg a$ and $D \gg b$.

The X -axis is used to identify each point on the screen. Each aperture, by itself, would generate the same single-slit diffraction pattern

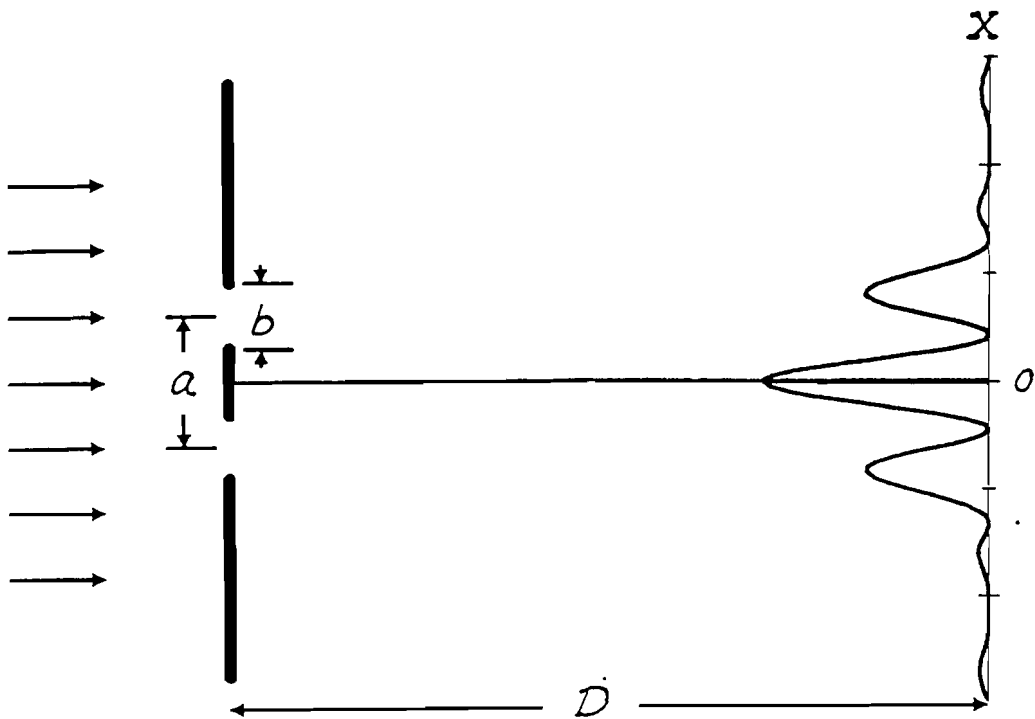


Figure 1. The double-slit geometry used in the theoretical calculation of the intensity pattern.

on the viewing screen. At any point on the screen the contributions from the two slits overlap coherently and interference must occur.

To obtain an expression for the optical disturbance at a point $P(x)$, we need to slightly reformulate the single-slit diffraction analysis. In the Fraunhofer approximation, the total contribution to the electric field at point $P(x)$ from both slits is,

$$E = C \int_{-b/2}^{b/2} F(z) dz + C \int_{a-b/2}^{a+b/2} F(z) dz, \quad (1)$$

where $F(z) = \sin[\omega t - k(R - z \sin \theta)]$, it is the contribution to the electric field at $P(x)$ from some point of either one of the two apertures. The constant amplitude factor C is the secondary source strength per unit length along the z axis divided by R , which is measured from the origin to the point $P(x)$. The source strength is assumed to be independent of z over each aperture and R is assumed to be constant. We will be concerned only with relative intensity along the X -axis, so that the actual value of C is not important. Integration of Equation 1 yields,

$$E = bC \left(\frac{\sin \beta}{\beta} \right) [\sin(\alpha t - kR) + \sin(\alpha t - kR + 2\alpha)], \quad (2)$$

with $\alpha \equiv (ka/2) \sin \theta$, $\beta \equiv (kb/2) \sin \theta$. This is just the sum of the two fields at $P(x)$, the distance from the first slit to $P(x)$ is R , giving a phase term equal to $(-kR)$. The distance from the second slit to $P(x)$ is $(R - a \sin \theta)$

or $(R - 2\alpha/k)$, yielding a phase term equal to $(-kR + 2\alpha)$, as in the second sine function. The quantity 2β is the phase difference between two nearly parallel rays, arriving at point $P(x)$ on the X -axis, from top and bottom edges of one of the slits. The quantity 2α is the phase difference between two waves arriving at $P(x)$, one having originated at any point in the first slit, the other coming from the corresponding point in the second slit. Simplifying Equation 2 a bit further, it becomes

$$E = 2bC\left(\frac{\sin \beta}{\beta}\right) \cos \alpha \sin(\omega t - kR + \alpha), \quad (3)$$

which when squared and averaged over a relatively long interval in time is the intensity function. The reason for averaging is that the response time for the detector τ is much greater than the vibrating period of the light wave, so what the detector records is the average intensity of one period. So the intensity is

$$I(\theta) = 4I_0\left(\frac{\sin^2 \beta}{\beta^2}\right) \cos^2 \alpha. \quad (4)$$

In the $\theta = 0$ direction (i.e., when $\beta = \alpha = 0$), I_0 is the flux-density contribution from either slit, and $I(0) = 4I_0$ is the total flux density. The factor of 4 comes from the fact that the amplitude of the electric field is twice what it would be at that point with one slit covered. This expression can be viewed as being generated by a $\cos^2 \alpha$ double-slit interference term modulated by a $(\sin^2 \beta)/\beta^2$ single-slit diffraction term.

At angular positions (θ -values) where $\beta = \pm\pi, \pm2\pi, \pm3\pi, \dots$, diffraction effects are such that no light reaches $P(x)$, and clearly none is available for interference. At points on $P(x)$ where $\alpha = \pm\pi/2, \pm3\pi/2, \pm5\pi/2, \dots$, the various contributions to the electric field will be completely out of phase and will cancel due to the double-slit interference, regardless of the actual amount of light made available from the diffraction process. That is quite different from what we will see later in the experiment data; we did not get value 0 at any point.

We used the Quattro Pro spreadsheet to calculate the theoretical diffraction intensity pattern. We chose parameters that appear to be close to the experiment so that we could compare the difference between them. The results are presented in Figure 2

2. Double-slit Diffraction Experiment

The experimental setup is just as shown in Figure 3, which is not to scale; it is just a demonstration. The 3-milliWatt HeNe Laser emits a parallel light beam which is incident on the screen of the double-slit. At a certain distance D the diffraction intensity is detected by the optical fiber bundle which is mounted on a sliding bench. The optical fiber bundle can be moved manually along the bench to scan across the whole diffraction pattern. The signal is first processed by the PASCO photo detector and then transferred to the computer. We use the Vernier data acquisition

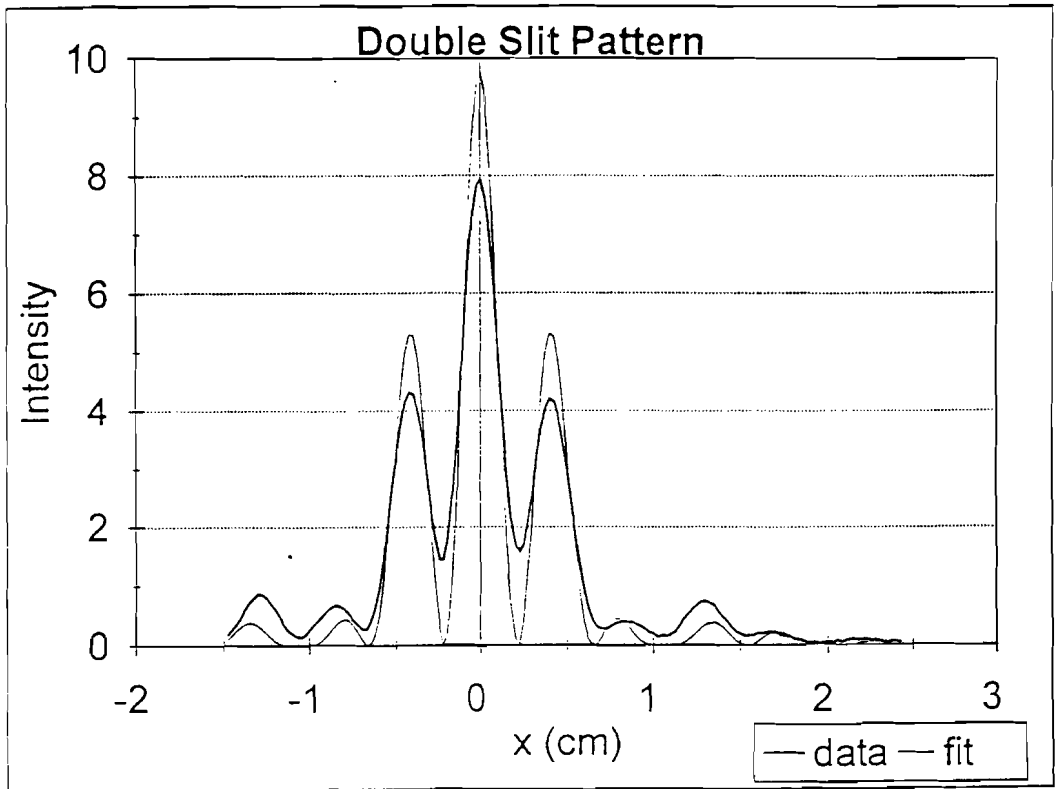


Figure 2. The theoretical double-slit diffraction pattern (thin line) and the data (thick line). The theoretical curve was generated using a slit separation $a=0.13$ cm and slit width $b=0.056$ cm which best fit the maxima and minima of the data. The intensity has arbitrary units in order to compare the two patterns

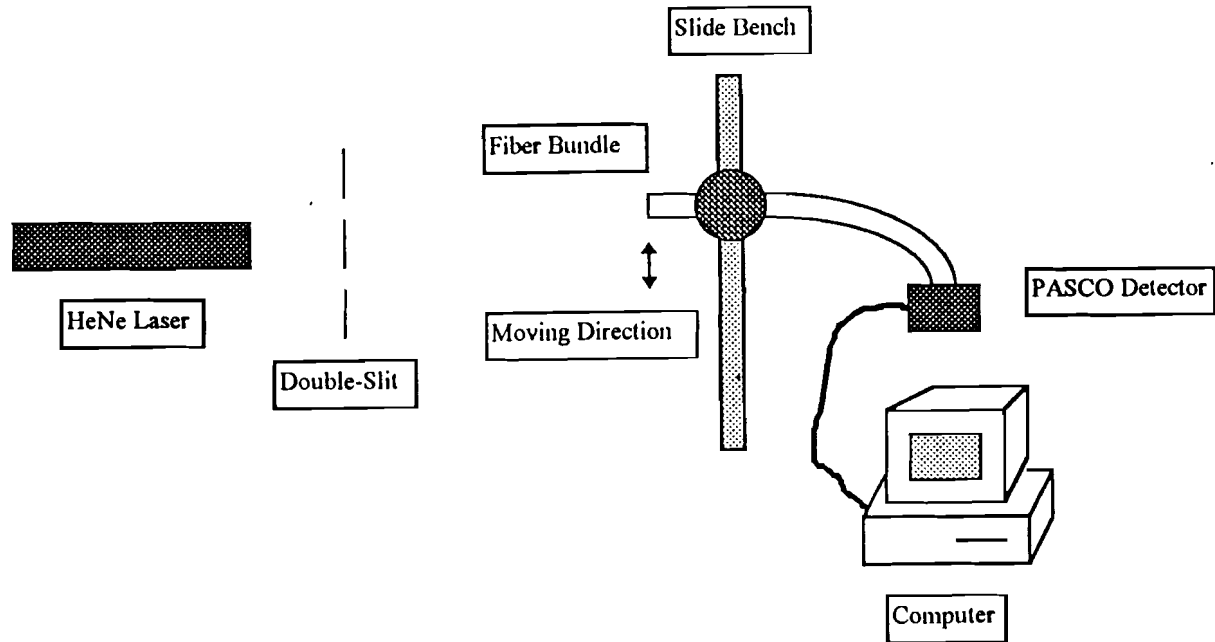


Figure 3. The setup for the double-slit diffraction experiment. The end of the optical fiber bundle detector can be moved manually along the sliding bench to scan across the diffraction pattern.

software known as Data Monitor⁸. The Quattro Pro spreadsheet is used to process the data.

The following data is what we obtained for our experiment:

Width of the slit of double-slit:	$b = 0.056 \text{ cm}$
Distance between the center of the two slits:	$a = 0.13 \text{ cm}$
Distance between the double-slit and the optical fiber bundle:	$D = 91.1 \text{ cm}$
Radius of the optical fiber bundle:	$R = 0.11 \text{ cm}$
Distance between the two measured data points:	$dy = 0.025 \text{ cm}$

We measured 157 points of the diffraction pattern which are plotted in the Figure 2. Comparing the measured data with the theoretical diffraction pattern, the measured data do not have minima zero points and the maxima are smaller than the corresponding maxima of the theoretical pattern, the minima are greater than the corresponding minima of the theoretical pattern.

As for the processing of the measured data by FFT later, we actually used 128 points of the measured data. As is discussed in Chapter 3, this is because the FFT method requires the number of data points to be 2^N .

Chapter 3

Fourier Analysis and Optimal Filtering Theory

1. Fourier Analysis

1.1 Completeness and Orthogonality of Sinusoidal Functions

⁴Jean Baptiste Joseph Fourier(1768-1830), the famous French mathematician presented this theorem that any periodic function of period 2π can be expressed in the form

$$f(t) = \frac{a_0}{2} + \sum_{n=1}^{\infty} a_n \cos nt + \sum_{n=1}^{\infty} b_n \sin nt. \quad (5)$$

For our purposes, we will assume the Fourier series converges for any problem of interest to us. At a mathematical level, the Fourier series works because the sines and cosines form a complete, orthogonal set. Completeness means they are sufficient to describe any periodic function as in Equation 5. The orthogonality is expressed by

$$\int_{-\pi}^{\pi} \sin mt \sin ntdt = \begin{cases} \pi\delta_{m,n}, & m \neq 0, \\ 0, & m = 0, \end{cases} \quad (6)$$

$$\int_{-\pi}^{\pi} \cos mt \cos nt dt = \begin{cases} \pi \delta_{m,n}, & m \neq 0, \\ 2\pi, & m = n = 0, \end{cases} \quad (7)$$

$$\int_{-\pi}^{\pi} \sin mt \cos nt dt = 0, \quad \text{all integral } m \text{ and } n. \quad (8)$$

Using these orthogonality relations, we can easily find that the coefficients are derived from the given function by the standard formulas

$$a_n = \frac{1}{\pi} \int_{-\pi}^{\pi} f(t) \cos nt dt, \quad (9)$$

and

$$b_n = \frac{1}{\pi} \int_{-\pi}^{\pi} f(t) \sin nt dt. \quad (10)$$

While much of our work will be with real functions, the concept of Fourier series is applicable to complex functions as well. Expressing the sines and cosines as exponentials, Equation 5 can be rewritten as

$$f(t) = \sum_{n=-\infty}^{\infty} c_n e^{int} \quad (11)$$

in which

$$c_n = \begin{cases} (a_n - ib_n) / 2, & n > 0, \\ a_n, & n = 0, \\ (a_{|n|} + ib_{|n|}) / 2, & n < 0, \end{cases} \quad (12)$$

The c_n 's can, of course, be obtained by integration,

$$c_n = \frac{1}{2\pi} \int_{-\pi}^{\pi} f(t) e^{-int} dt. \quad (13)$$

1.2 The Fourier Transform

Closely related to the idea of the Fourier series representation of a function is the Fourier transform of a function. The series representation is useful in describing functions over a limited region, or on the infinite interval $(-\infty, \infty)$ if the function is periodic. Fourier transforms, on the other hand, are useful in describing nonperiodic functions on the infinite interval.

To develop the transform, first consider the series representation of a function that is periodic on the interval $[-T, T]$. Making the substitution $t = \pi t/T$, we have

$$f(t) = \sum_{-\infty}^{\infty} c_n e^{in\pi/T}, \quad (14)$$

where

$$c_n = \frac{1}{2T} \int_{-T}^T f(t) e^{-in\pi/T} dt. \quad (15)$$

We can now identify the discrete frequencies appearing in the summations as being

$$\omega = \frac{n\pi}{T}, \quad (16)$$

and the differences between successive frequencies as being

$$\Delta\omega = \frac{\pi}{T}. \quad (17)$$

Then the series can be written as

$$f(t) = \sum_{-\infty}^{\infty} c_n e^{in\Delta\omega t}, \quad (18)$$

where

$$c_n = \frac{\Delta\omega}{2\pi} \int_{-T}^T f(t) e^{-in\Delta\omega t} dt. \quad (19)$$

We now define

$$c_n = \frac{\Delta\omega}{\sqrt{2\pi}} g(n\Delta\omega) \quad (20)$$

so that

$$g(n\Delta\omega) = \frac{1}{\sqrt{2\pi}} \int_{-T}^T f(t) e^{-in\Delta\omega t} dt \quad (21)$$

and

$$f(t) = \frac{1}{\sqrt{2\pi}} \sum_{n=-\infty}^{\infty} \Delta\omega g(n\Delta\omega) e^{in\Delta\omega t}. \quad (22)$$

We now take the limit as $T \rightarrow \infty$. In so doing, $n\Delta\omega$ becomes the continuous variable ω and the summation in Equation 21 becomes an integral. Therefore

$$f(t) = \frac{1}{\sqrt{2\pi}} \int_{-\infty}^{\infty} g(\omega) e^{i\omega t} d\omega \quad (22)$$

and

$$g(\omega) = \frac{1}{\sqrt{2\pi}} \int_{-\infty}^{\infty} f(t) e^{-i\omega t} dt. \quad (23)$$

Now define $g(\omega)$ to be the Fourier transform of $f(t)$,

$$\mathcal{F}[f(t)] = g(\omega) = \frac{1}{\sqrt{2\pi}} \int_{-\infty}^{\infty} f(t) e^{-i\omega t} dt. \quad (24)$$

and $f(t)$ to be the inverse transform of $g(\omega)$,

$$\mathcal{F}^{-1}[g(\omega)] = f(t) = \frac{1}{\sqrt{2\pi}} \int_{-\infty}^{\infty} g(\omega) e^{i\omega t} d\omega. \quad (25)$$

1.3 The Discrete Fourier Transform

⁷When a physical quantity is a function of time it is measured in discrete time increments of Δt . As a result, we have a discrete set of numbers $f(m\Delta t)$, $m = 0, 1, \dots, N-1$. Under these conditions, we cannot actually calculate the true Fourier transform using Equation 23 since we do not have enough data to work with. We do not have any data before $t = 0$, and do not have continuous data, but only data at times $m\Delta t$.

However we can calculate something that resembles the Fourier transform. We will assume we took data for a sufficiently long time T that all the interesting behavior is contained in the data available. We can approximate the Fourier transform of the true data over an infinite range by something resembling a Fourier series representation of the actual data, on the interval $0 < t < T$.

The complex representation of the Fourier series on the interval $0 < t < T$ can be written as

$$f(t) = \sum_{-\infty}^{\infty} c_n e^{i2\pi nt/T}, \quad (26)$$

with the coefficients given by the integral

$$c_n = \frac{1}{T} \int_0^T f(t) e^{-i2\pi nt/T} dt. \quad (27)$$

This representation of the function is periodic with period T . In order to make this more like a Fourier transform, define

$$\Delta\omega = \frac{2\pi}{T}. \quad (28)$$

We then approximate the integral by the trapezoidal rule, and define the discrete Fourier transform as

$$g(n\Delta\omega) = \sum_{m=0}^{N-1} f(m\Delta t) e^{-in\Delta\omega m\Delta t} = \sum_{m=0}^{N-1} f(m\Delta t) e^{-i2\pi mn/N}. \quad (29)$$

Since we only have N known quantities, the data taken at N times, we can only determine the transform at N frequencies.

As for evaluating the inverse transform, we can find an exact inversion procedure based on the idea of orthogonality. Consider the idea that functions can be orthogonal to one another, in the sense of performing an integration. They can also be orthogonal in the sense of a summation.

Consider the sum

$$S_n = \sum_{k=0}^{N-1} e^{ik\alpha} = \frac{1 - e^{i\alpha N}}{1 - e^{i\alpha}} \quad (30)$$

In order to generate an orthogonality relation, we need to find a way to force S_n to be zero if $\alpha \neq 0$. We can do this by requiring that

$$e^{i\alpha N} = 1, \quad (31)$$

or that

$$\alpha = 2\pi l / N \quad (32)$$

with l an integer. This makes $1 - e^{i\alpha N}$, and hence S_N , zero. We can then write

$$\sum_{k=0}^{N-1} e^{i2\pi k l / N} = \begin{cases} N, & l = 0 \\ 0, & l \neq 0 \end{cases} \quad (33)$$

We now express l as the difference between the two integers m and n , and find our orthogonality relation

$$\sum_{k=0}^{N-1} e^{i2\pi km/N} e^{-i2\pi kn/N} = N\delta_{m,n}. \quad (34)$$

Returning to the DFT given by Equation 29, multiply both sides by $e^{i2\pi kn/N}$ and summing over n to find

$$\begin{aligned} \sum_{n=0}^{N-1} g(n\Delta\omega) e^{i2\pi kn/N} &= \sum_{n=0}^{N-1} \sum_{m=0}^{N-1} f(m\Delta t) e^{-i2\pi mn/N} e^{i2\pi kn/N} \\ &= \sum_{m=0}^{N-1} f(m\Delta t) \sum_{n=0}^{N-1} e^{-i2\pi mn/N} e^{i2\pi kn/N} \\ &= \sum_{m=0}^{N-1} f(m\Delta t) N\delta_{k,m} \\ &= Nf(k\Delta t). \end{aligned} \quad (35)$$

The inverse discrete Fourier transform is then given as

$$f(m\Delta t) = \frac{1}{N} \sum_{n=0}^{N-1} g(n\Delta\omega) e^{i2\pi mn/N}. \quad (36)$$

The discrete Fourier transform is different from the Fourier transform, for example, the DFT uses only finite summations in its evaluations. It also has considerable computational advantage over the Fourier transform in practical problems.

1.4 Fast Fourier Transform

The discrete Fourier transform is a powerful tool in mathematical physics, but it is still a computationally intensive operation.⁷ With N data points, there will be on the order of N operations performed in each summation. And this only yields one data point in ω -space. To evaluate all the $g(m\Delta\omega)$, we'll need to perform N summations, for a total of N^2 operations. So, if we double the number of points, we quadruple the effort necessary to perform the calculation.

Fourier analysis is a premier tool of the computational physicist because of the existence of a streamlined calculational procedure, the fast Fourier transform FFT. If N is an even number, then we can write the DFT as a sum over even-numbered points and a sum over odd-numbered points:

$$\begin{aligned}
 g(n\Delta\omega) &= \sum_{m=0}^{N-1} f(m\Delta t) e^{-i2\pi mn/N} \\
 &= \sum_{m=0, \text{even}}^{N-1} f(m\Delta t) e^{-i2\pi mn/N} + \sum_{m=0, \text{odd}}^{N-1} f(m\Delta t) e^{-i2\pi mn/N} \quad (37) \\
 &= \sum_{j=0}^{N/2-1} f(2j\Delta t) e^{-i2\pi 2jn/N} + \sum_{j=0}^{N/2-1} f((2j+1)\Delta t) e^{-i2\pi(2j+1)n/N},
 \end{aligned}$$

where we've let $m = 2j$ in the first term (even points), and $m = 2j + 1$ in the second term (odd points). But this is simply

$$\begin{aligned}
g(n\Delta\omega) &= \sum_{j=0}^{N/2-1} f(2j\Delta t)e^{-i2\pi jn/(N/2)} \\
&\quad + e^{-i2\pi n/N} \sum_{j=0}^{N/2-1} f((2j+1)\Delta t)e^{-i2\pi jn/(N/2)} \\
&= g_{\text{even}}(n\Delta\omega) + e^{-i2\pi n/N} g_{\text{odd}}(n\Delta\omega),
\end{aligned} \tag{38}$$

we can see that sums are themselves DFTs, with half as many points, over the original even- and odd-numbered points. The original calculation of the DFT was to take on the order of N^2 operations, but this decomposition shows that it actually only requires $2 \times (N/2)^2$ operations. If we don't stop, each of these DFTs can be decomposed into even and odd points, and so on, as long as they each contain an even number of points. Let's say that $N = 2^k$, then after k steps there will be N transforms to be evaluated, each containing only one point! The total operation count is thus not on the order of N^2 , but rather on the order of $N \log_2 N!$. The fast Fourier transform is fast.

The Quattro Pro spreadsheet has the FFT built-in function. We use that function to process our data.

2. Convolution and Deconvolution Theorem

⁷Consider two functions, $f(x)$ and $h(x)$. Mathematically, the convolution of the two functions can be defined as

$$g \equiv f \otimes h = \int_{-\infty}^{\infty} f(x)h(x-X)dx . \quad (39)$$

In Section 1 we discussed Fourier analysis in the time (t) and frequency (ω) domains. Although they are actually equivalent, we use position (x) and wave number (k) domains in order to explain our situation more clearly.

Here g is defined as the convolution of f and h . Convolution can have different physical meanings for different applications. As for our case, f represents the input function to the detector, h represents the response function of the detector, and g represents the output function from the detector.

The detecting cross section of our optical fiber bundle detector is not an ideal infinitesimal point. The receiving signal at each point actually adds up all the contributions incident on the cross section which covers some amount of area, so it can not represent the real signal at that point. The convolution actually is the description of this kind of weighted summation. The h can be regarded as a weight function. We will give a model of h for our case in Chapter 4. In one word, we can say that convolution is the mathematical description of the physical distortion of the input.

Now consider the Fourier transform of the convolution,

$$\mathcal{F}[f \otimes h] = \frac{1}{\sqrt{2\pi}} \int_{-\infty}^{\infty} [f \otimes h] e^{-ikx} dx \quad (40)$$

$$\begin{aligned}
&= \frac{1}{\sqrt{2\pi}} \int_{-\infty}^{\infty} \left[\frac{1}{\sqrt{2\pi}} \int_{-\infty}^{\infty} f(X)h(x-X)dX \right] e^{-ikx} dx \\
&= \frac{1}{\sqrt{2\pi}} \int_{-\infty}^{\infty} f(X) \left[\frac{1}{\sqrt{2\pi}} \int_{-\infty}^{\infty} h(x-X)e^{-ikx} dx \right] dX.
\end{aligned}$$

We can define $w = x - X$, and make the substitution $x = w + X$. After rearranging the integrals, we get

$$\begin{aligned}
\mathcal{F}[f \otimes h] &\equiv G(k) = \left[\frac{1}{\sqrt{2\pi}} \int_{-\infty}^{\infty} f(X)e^{-ikX} dX \right] \cdot \left[\frac{1}{\sqrt{2\pi}} \int_{-\infty}^{\infty} h(w)e^{-ikw} dw \right] \\
&= F(k) \cdot H(k),
\end{aligned} \tag{41}$$

where

$$F(k) \equiv \mathcal{F}[f(x)] = \frac{1}{\sqrt{2\pi}} \int_{-\infty}^{\infty} f(x)e^{-ikx} dx, \tag{42}$$

and

$$H(k) \equiv \mathcal{F}[h(x)] = \frac{1}{\sqrt{2\pi}} \int_{-\infty}^{\infty} h(x)e^{-ikx} dx. \tag{43}$$

This is known as the Fourier Convolution Theorem which is very useful in calculating convolutions.

While there are instances where we want the convolution, we are often more interested in the deconvolution. That is, if we know the measured data $g(x)$, can we find the $f(x)$ which is the uncorrupted original input function and try to eliminate the effect of the detector? Using deconvolution we can do that.

From the convolution theorem equation (41), we can get

$$F(k) = \frac{G(k)}{H(k)}, \quad (44)$$

then by applying the inverse Fourier transform, we get

$$f(x) = \mathcal{F}^{-1} \left[\frac{G(k)}{H(k)} \right]. \quad (45)$$

This useful result is what deconvolution can give us.

3. Optimal (Wiener) Filtering

According to the discussion above, we can deconvolve the effect of the response function with the detector h in the absence of any noise. In practice the presence of noise degrades the signal beyond the effect of the detector response. It is necessary to develop a technique to handle this situation. Optimal filtering is a very effective tool to be used to remove the noise from a corrupted signal.

⁶The measured data contains an additional component of noise. We define the measured data $c(x)$, including the effect of noise by,

$$c(x) = g(x) + n(x) \quad (46)$$

where $g(x)$ is the data without noise and $n(x)$ is the noise term.

The removal of the effect of noise can be discussed by using Fourier transforms. Since we need to apply the optimal filtering in wave number (k) domain, the Fourier transform should be applied to $c(x)$, $g(x)$ and $n(x)$.

$$C(k) = \frac{1}{\sqrt{2\pi}} \int_{-\infty}^{\infty} c(x)e^{-ikx} dx \quad (47)$$

$$G(k) = \frac{1}{\sqrt{2\pi}} \int_{-\infty}^{\infty} g(x)e^{-ikx} dx \quad (48)$$

$$N(k) = \frac{1}{\sqrt{2\pi}} \int_{-\infty}^{\infty} n(x)e^{-ikx} dx . \quad (49)$$

Then in wave number (k) domain we get

$$C(k) = G(k) + N(k) . \quad (50)$$

The main goal of optimal filtering is to find the optimal filter $\Phi(k)$ which when applied to the measured data $C(k)$ (notice it already contains noise), produces a quantity $\tilde{G}(k)$ which is a reasonable approximation to the noiseless transform $G(k)$. Then $\tilde{G}(k)$ can be deconvolved with $H(k)$ according to Equation 44 to produce a quantity $\tilde{F}(k)$ that is a reasonable approximation to the uncorrupted transform $F(k)$. In other words we will calculate

$$\tilde{G}(k) = C(k)\Phi(k) \quad (51)$$

and

$$\tilde{F}(k) = \tilde{G}(k) / H(k) \quad (52)$$

i.e.

$$\tilde{F}(k) = \frac{\Phi(k)C(k)}{H(k)}. \quad (53)$$

Then we can calculate an approximation to the uncorrupted signal by taking the inverse transform

$$\tilde{f}(x) = \mathcal{F}^{-1}[\tilde{F}(k)]. \quad (54)$$

We demand that $\tilde{F}(k)$ be close to $F(k)$ in the least-square sense; that means

$$\int_{-\infty}^{\infty} \left| \tilde{F}(k) - F(k) \right|^2 dk \quad \text{is minimized.} \quad (55)$$

Substituting Equations 44, 50 and 53, Equation 55 becomes

$$\begin{aligned} & \int_{-\infty}^{\infty} \left| \frac{[G(k) + N(k)]\Phi(k)}{H(k)} - \frac{G(k)}{H(k)} \right|^2 dk \\ &= \int_{-\infty}^{\infty} |H|^{-2} \left\{ |G + N|^2 |\Phi|^2 + |G|^2 - 2|G + N| \cdot |\Phi| \cdot |G| \right\} dk \\ &= \int_{-\infty}^{\infty} |H|^{-2} \left\{ [|G|^2 + 2|G| \cdot |N| + |N|^2] \cdot |\Phi|^2 + |G|^2 - 2|G|^2 |\Phi| - 2|N| \cdot |G| \cdot |\Phi| \right\} dk \\ &= \int_{-\infty}^{\infty} |H|^{-2} \left\{ |G|^2 |1 - \Phi|^2 + |N|^2 |\Phi|^2 \right\} dk . \end{aligned} \quad (56)$$

According to Reference 6, the signal G and the noise N are uncorrelated; this means that their cross product, when integrated over wave number k , gives nearly zero. This can be used as a definition of noise. Obviously Equation 56 will be a minimum if and only if the integrand is minimized with respect to $\Phi(k)$ at every value of k . This is a problem in the calculus of variations. Consider $\Phi(k)$ to be a real function. Differentiating with respect to Φ and setting the result equal to zero gives

$$|H|^{-2} \left\{ -2|G|^2 |1 - \Phi| + 2|N|^2 |\Phi| \right\} = 0 \quad (57)$$

and then we get

$$\Phi(k) = \frac{|G(k)|^2}{|G(k)|^2 + |N(k)|^2}. \quad (58)$$

This is the formula for the optimal or Wiener filter $\Phi(k)$.

Notice that Equation 58 does not contain $F(k)$, the true signal. This allows an important simplification: The optimal filter can be determined independently of the determination of the deconvolution function that relates $F(k)$ and $G(k)$.

To determine the optimal filter from Equation 58 we need some way of separately estimating $|G|^2$ and $|N|^2$. There is no way to do this from the measured signal C alone without some other information, or some assumption. Since the optimal filter results from a minimization problem, the quality of the results obtained by optimal filter is second order in the precision to which the optimal filter is determined. In practice, even a fairly crudely determined optimal filter can give excellent results when it is

applied to data. So we can make a reasonable hypothesis as to what the optimal filter is by examining $C(k)$, the Fourier transform of the raw data. Draw a smooth curve through the noise spectrum, extrapolating it into the region dominated by the signal as well. Then draw a smooth curve through the signal plus noise power. The difference between these two curves is the smooth model of the noiseless signal. Notice that from Equation 58 the $\Phi(k)$ will be close to unity where the noise is negligible, and close to zero where the noise is dominant. The intermediate dependence given by the filter is the optimal way of interpolating between these two extremes.

Chapter 4

Results

1. The Theoretical and Experimental Results of Double-slit Diffraction Pattern.

Using the Fraunhofer diffraction theory of the double-slit as discussed in Chapter 2, we obtained the theoretical curve of the double-slit diffraction pattern as shown in Figure 2. Using the optical fiber bundle detection system as shown in Figure 3, we obtained the experimental data and plotted it along with the theoretical curve in Figure 2. The minima and maxima are at the same locations. As for the differences, the theoretical data has minima zeros, but the experimental data does not have, the maxima of the experimental data are smaller and the minima of the experimental data are greater for the three peaks. These differences are present because the noise gives the experimental data an offset and the averaging effect of the detector smears out the input signal.

2. The Model of Response Function $h(x)$.

2.1. The design of response function $h(x)$.

When the detector moves along the bench measuring the intensity of every point, the optical fiber bundle detector takes in all the energy incident on its cross section. We assume the cross section is circular and the intensity depends only on x . From Figure 4 the energy incident on the gray band can be calculated by multiplying $2\sqrt{R^2 - x^2} \cdot dx$ (the area of the gray band) and the intensity $I(x)$, so the total energy the detector actually records is the integral $\int_0^{2R} 2\sqrt{R^2 - x^2} \cdot I(x) \cdot dx$. This $\sqrt{R^2 - x^2}$ is just the response function $h(x)$ that we need, it characterizes the weighted response of the detector. Figure 5 shows the theoretical diffraction pattern and $h(x)$. Figure 6 shows the experimental data and $h(x)$.

2.2. The test of the model of $h(x)$.

The result of convolution of the theoretical double-slit diffraction pattern and response function $h(x)$ using the model we designed is shown in Figure 7 along with the measured data. The two curves are closely matched which means that the model of $h(x)$ works very well. In Figure 8, the theoretical double slit diffraction pattern is compared with what has been convoluted by the $h(x)$.

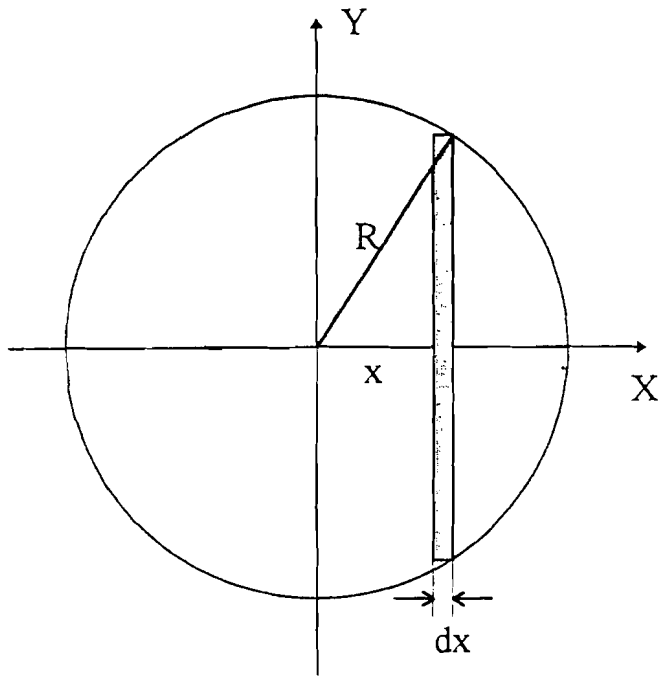


Figure 4. The calculation of model of the response function $h(x)$. The cross section of the end of the optic fiber detector is assumed to be circular with radius R .

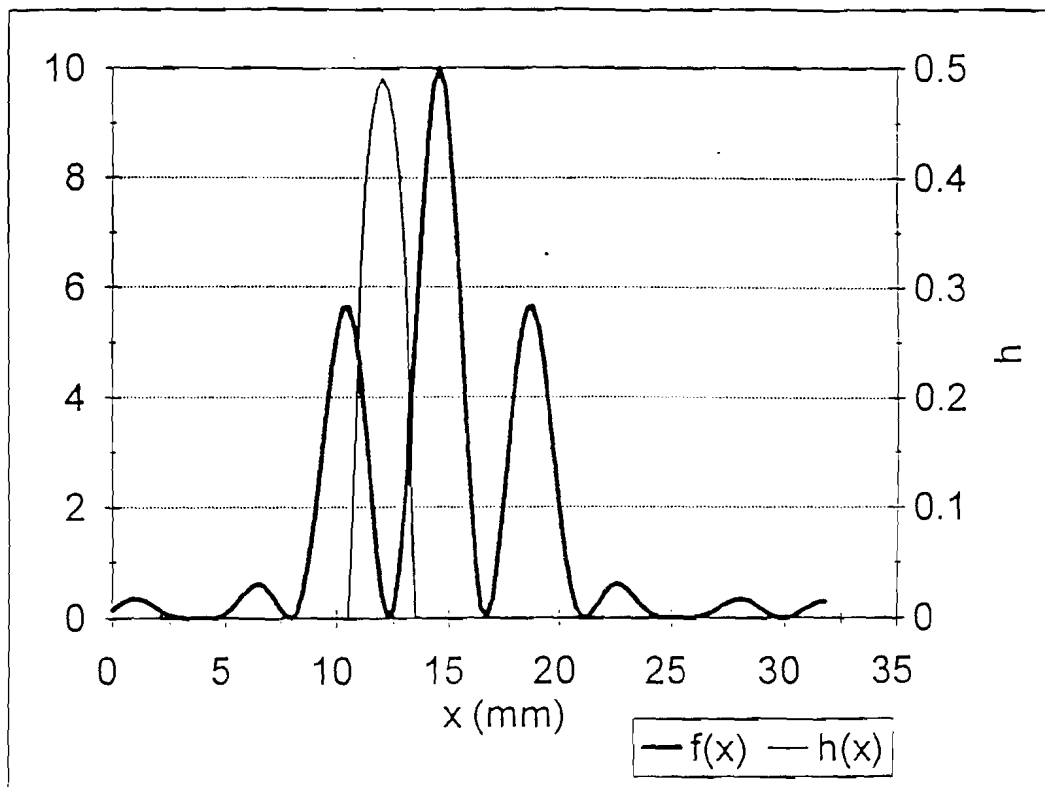


Figure 5. The response function $h(x)$ and the theoretical double-slit diffraction pattern.

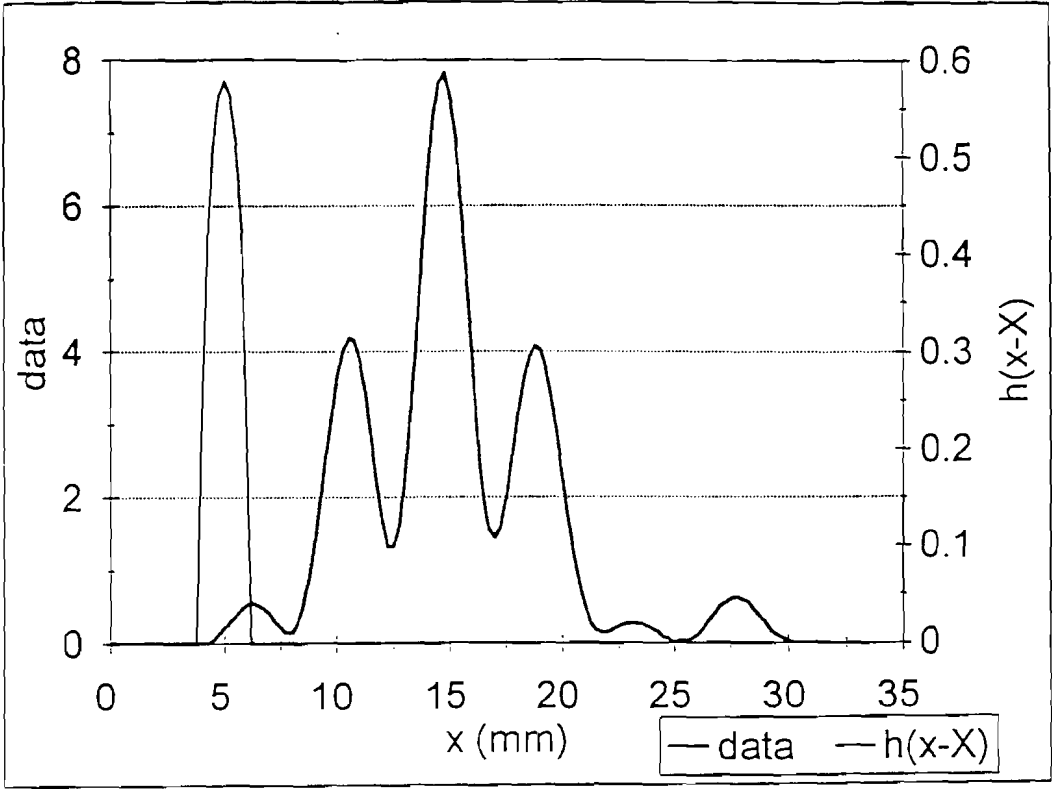


Figure 6. The response function $h(x)$ and the measured experimental data of the double-slit diffraction pattern.

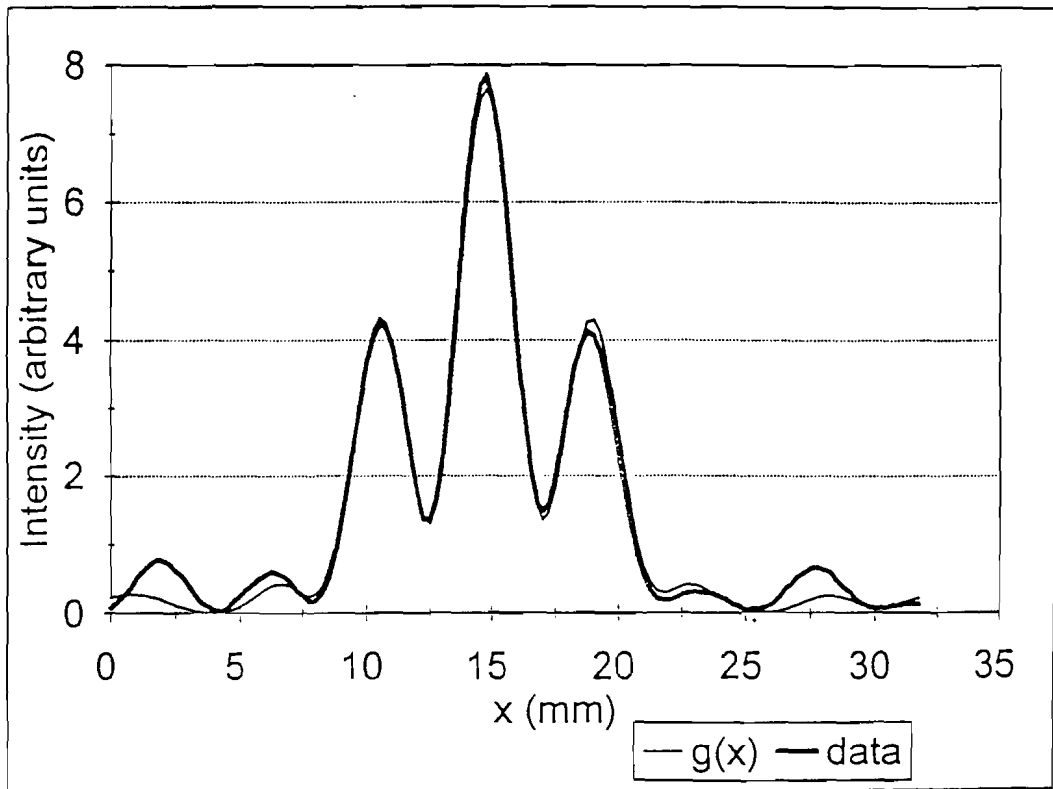


Figure 7. The thin curve is the theoretical double-slit diffraction pattern convolved with the response function $h(x)$. The thick curve is the measured experimental data.

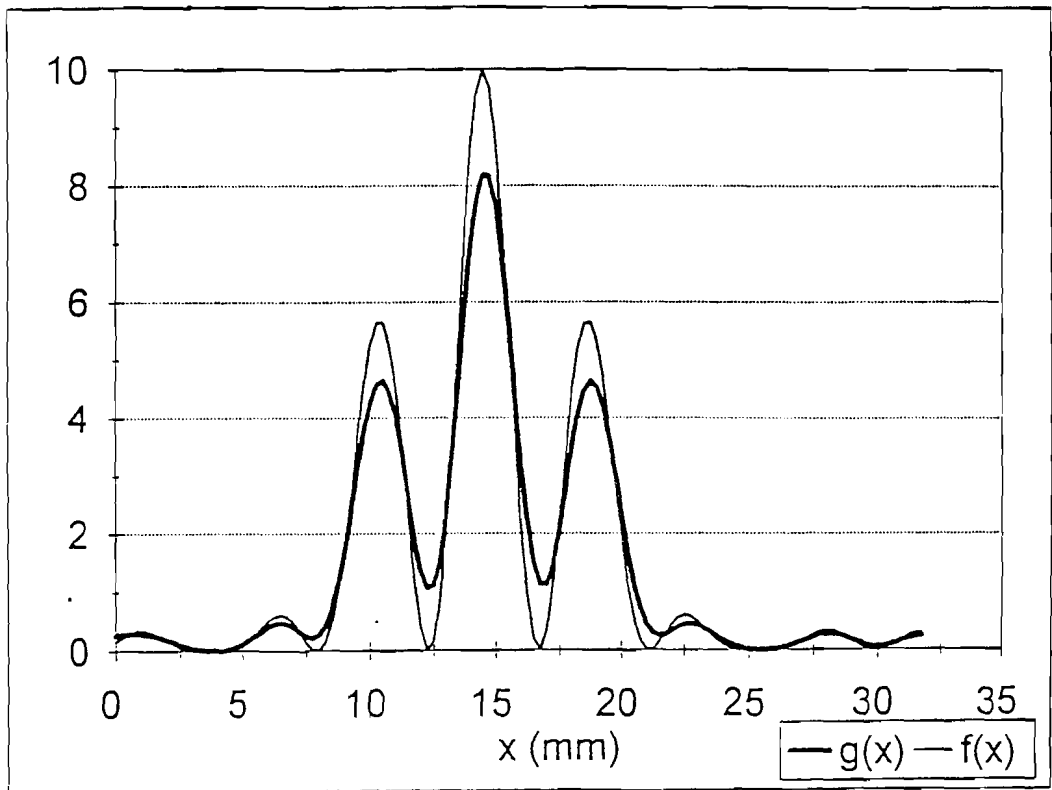


Figure 8. The thick curve is the theoretical double-slit diffraction pattern convolved with the response function $h(x)$. The thin curve is the theoretical double-slit diffraction pattern before convolution.

3. The Optimal Filter

3.1. The necessity of applying the optimal filter.

First we applied the deconvolution method to the measured data directly trying to get the uncorrupted signal pattern, but the result is far from the theoretical double-slit diffraction pattern. Because the process of deconvolution actually is quite sensitive to noise in the input data, it can sometimes produce poor results for this reason. So we have to apply the optimal filter method to eliminate the noise.

3.2. The estimation of G and N.

We first generate a theoretical $G(k)^2$ to compare with the measured data $C(k)^2$ in Figure 9. This gives us an idea of the difference between the two curves which is caused by noise. Then we used the method discussed in Chapter 4. We assume the values of $G(k)^2$ and $N(k)^2$ just as shown in the Figure 10.

3.3. The calculation of the filter.

After calculation using Equation 58, we get the optimal filter $\Phi(k)$ and plot $\Phi(k)^2 \cdot |C(k)|^2$ on the same graph as shown in Figure 11. We can see how the optimal filter works: When k is less than 0.25, $\Phi(k)$ is one and $\Phi(k)^2 \cdot |C(k)|^2$ is equal to $|C(k)|^2$; this part of the data is not modified.

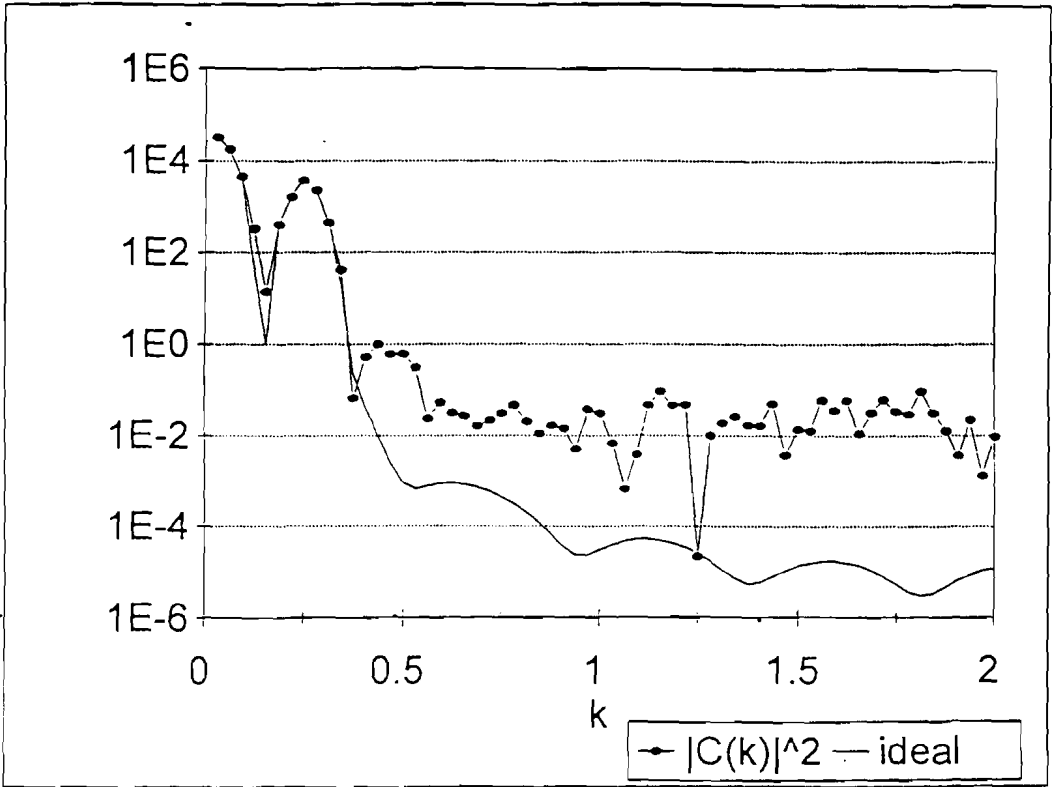


Figure 9. The thin curve is the square of $G(k)$, the Fourier transform of $g(x)$, which is the theoretical double-slit diffraction pattern convolved with the response function $h(x)$. The dots represent the square of $C(k)$, the Fourier transform of measured experimental data of double-slit diffraction pattern.

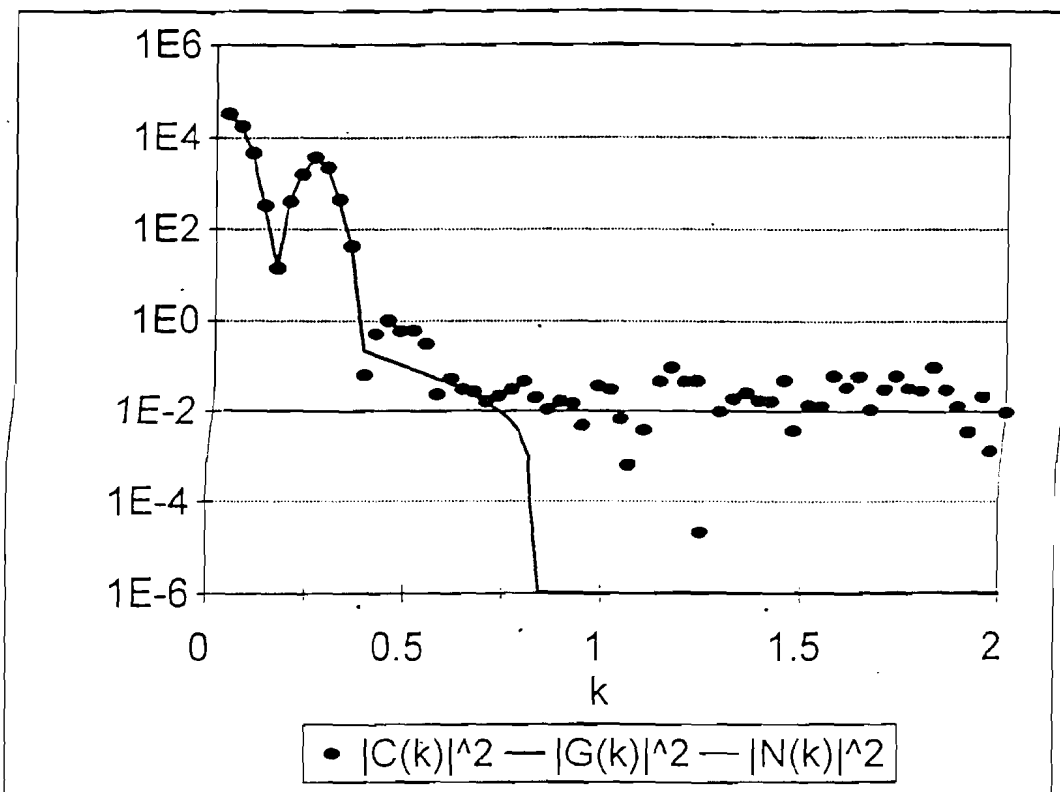


Figure 10. The dots represent the square of the Fourier transform of measured experimental data of double-slit diffraction pattern. The solid curve is the square of $G(k)$, the Fourier transform of model for the noiseless signal $g(x)$. The straight line is the square of $N(k)$, the Fourier transform of the model of noise $n(x)$.

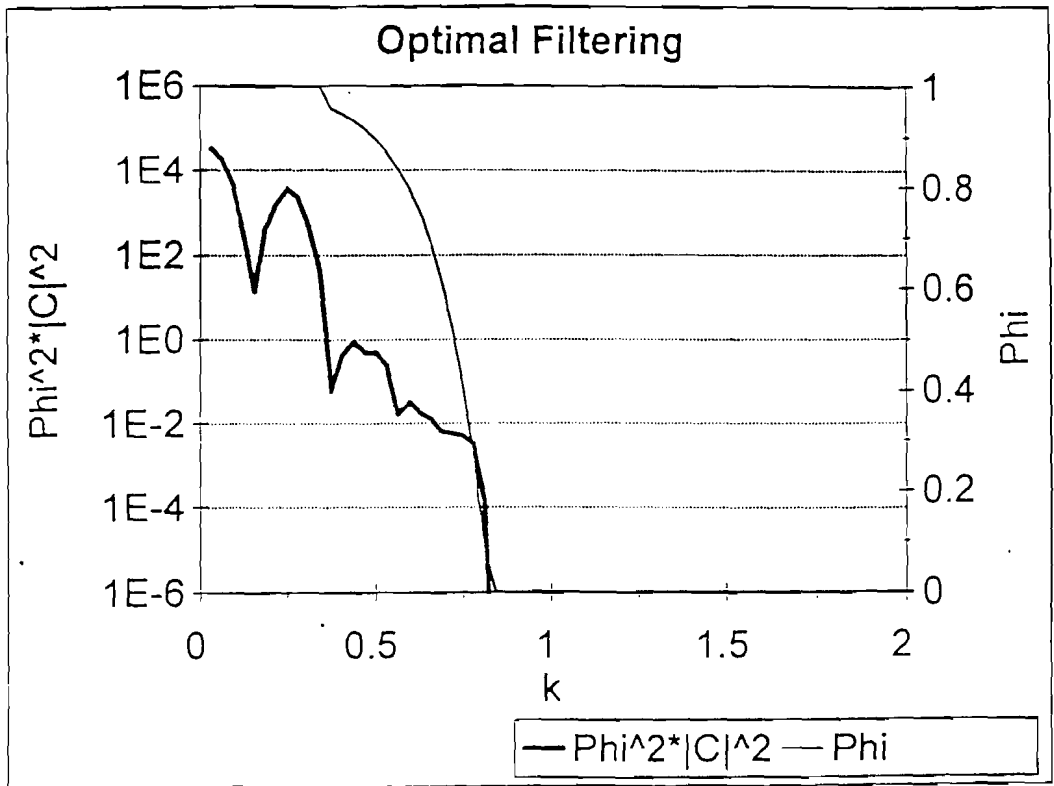


Figure 11. The thin curve is the optimal filter. The thick curve is the data after filtering.

When k is more than 1, $\Phi(k)$ is equal to zero, $\Phi(k)^2 \cdot |C(k)|^2$ is equal to zero, the noise in the data is successfully eliminated.

4. The Final Result

Using the Equation 53, we can get $\tilde{F}(k)$ and then take the inverse Fourier transform to get the final result $\tilde{f}(x)$ from which has been eliminated both the effect of response of the optical fiber bundle detector and the noise. In Figure 12 we compare the measured data with $\tilde{f}(x)$. In Figure 13 the theoretical double-slit diffraction pattern is compared with $\tilde{f}(x)$ which is the experimental measured data after filtering and deconvolution. The agreement between the theoretical curve and the data has been clearly improved.

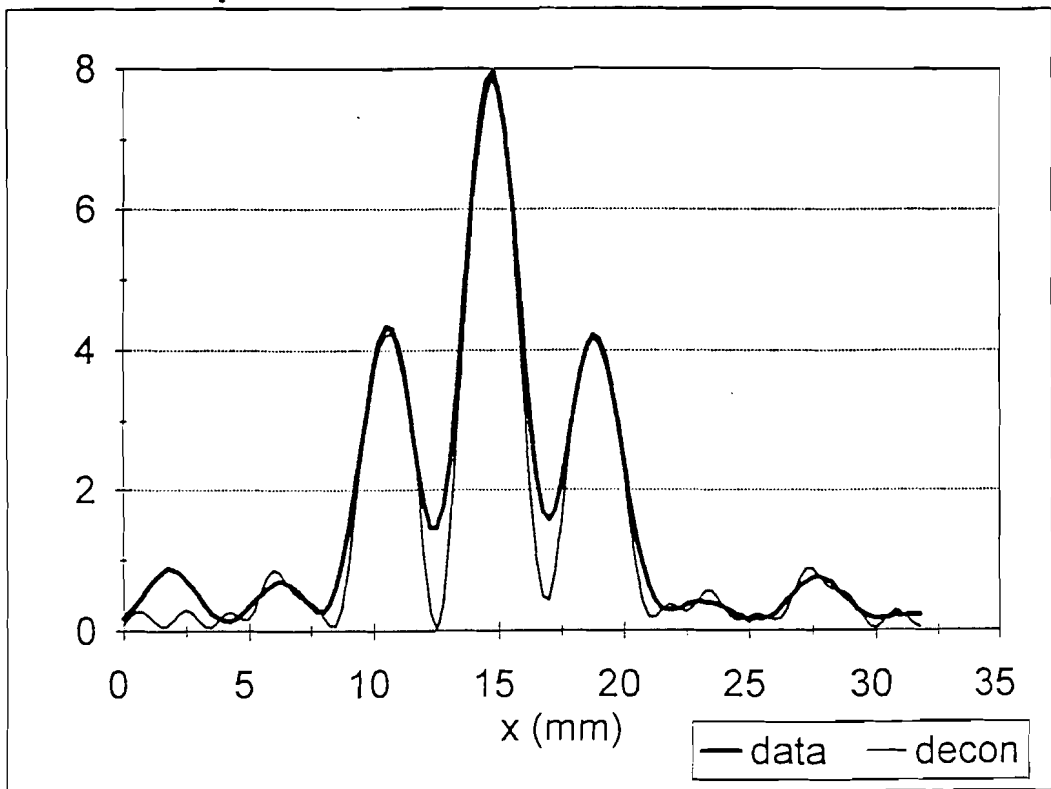


Figure 12. The thick curve is the measured experimental data of double-slit diffraction pattern. The thin curve is the measured experimental data after optimal filtering and deconvolution. The intensity has arbitrary units.

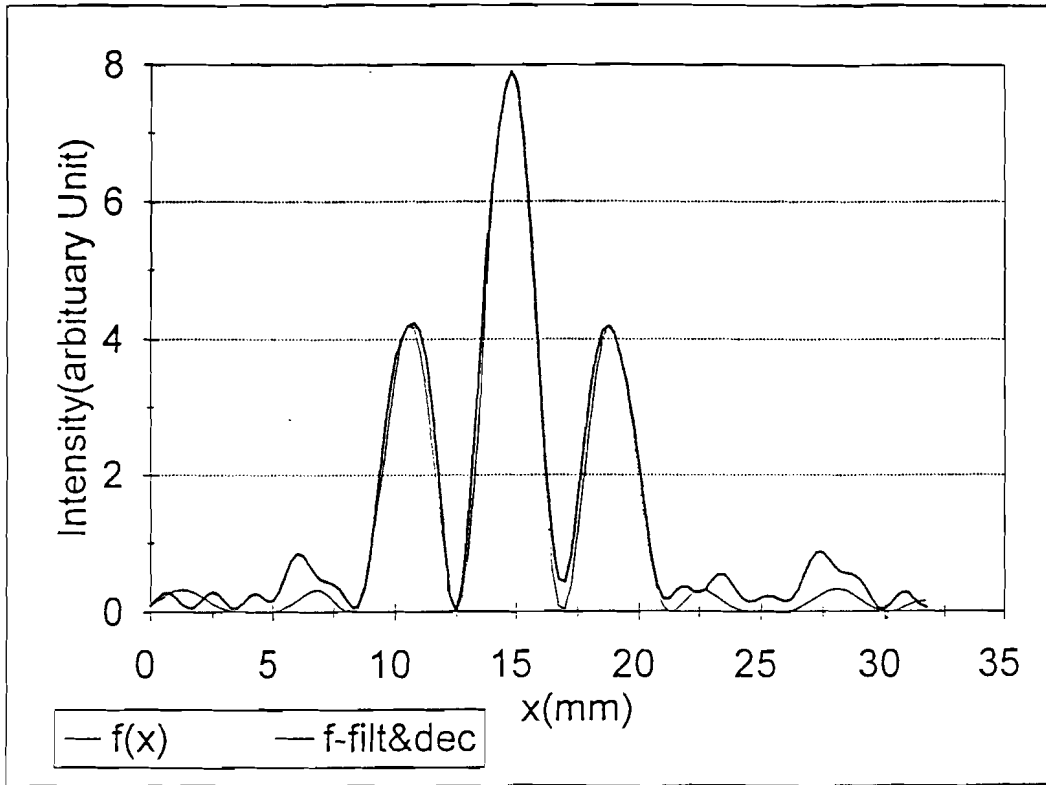


Figure 13. The thin curve is the theoretical double-slit diffraction pattern. The thick curve is the measured experimental data after optimal filtering and deconvolution. The intensity has arbitrary units.

Chapter 5

Conclusions

The optical fiber bundle detection system works well. The optimal filtering deconvolution method is feasible. By using this method we can actually detect the details of the pattern that are smaller than the cross section of the detector as long as we take enough data and have reasonable models of the response function and the noise. This is an important and very useful technique to get higher resolution by using the same detection system.

There are two points that need to be improved in the future. First, the existing system should be optimized. In order to be able to measure the data in more detail, we need greater intensity and higher resolution. Greater intensity will make the noise relatively small and easy to detect, and higher resolution is helpful in identifying detailed structure. However, intensity and resolution are two quantities related to each other. If we try to get more intensity we will lose some resolution and vice versa. So how to arrange the distance between the double-slit and the detector to create an optimized condition still needs to be investigated. Second, the collection of data should be automated. Since we move the detector along the slide bench manually, it takes a long time to get the data. This should be improved later.

REFERENCES

1. R. G. Wilson, *Fourier Series and Optical Transform Techniques in Contemporary Optics* (Wiley, New York, 1995).
2. E. Hecht, *Optics, Second Edition* (Addison-Wesley, Reading, 1987).
3. R. C. Gonzalez and R. E. Woods, *Digital Image Processing* (Addison-Wesley, Reading, 1992).
4. M. L. Boas, *Mathematical Methods in the Physical Sciences, Second Edition* (Wiley, New York, 1983).
5. F. L. Pedrotti and L. S. Pedrotti, *Introduction to Optics, Second Edition* (Prentice Hall, Englewood Cliffs, 1993).
6. W. H. Press and S. A. Teukolsky and W. T. Vetterling and B. P. Flannery, *Numerical Recipes in FORTRAN, Second Edition* (Cambridge University Press, 1992).
7. P. L. DeVries, *A First Course in Computational Physics* (Wiley, New York, 1994)
8. Vernier Software, *PASCO Scientific Data Monitor, Version 3/18/94*.

I, Kebin Li, hereby submit this thesis to Emporia State University as partial fulfillment of the requirement for an advanced degree. I agree that the Library of the University may make it available for use in accordance with its regulations governing materials of this type. I further agree that quoting, photocopying, or other reproduction of this document is allowed for private study, scholarship (including teaching) and research purposes of a nonprofit nature. No copying which involves potential financial gain will be allowed without written permission of the author.

Kebin Li

Signature of Author

May 8, 1996

Date

Convolution and Optimal Filtering in a
Fiber Optic Detection System

Title of Thesis

Dana Cooper

Signature of Graduate Office

Staff Member

May 8, 1996

Date Received